Journal of Hazardous Materials 177 (2010) 399–406

Contents lists available at ScienceDirect

Journal of Hazardous Materials

journal homepage: www.elsevier.com/locate/jhazmat

Effect of dissolved ozone or ferric ions on photodegradation of thiacloprid in presence of different TiO_2 catalysts

Urh Černigoj [a,*], Urška Lavrenčič Štangar [a], Jaromír Jirkovský [b]

[a] Laboratory for Environmental Research, University of Nova Gorica, Vipavska 13, SI-5001 Nova Gorica, Slovenia
[b] Heyrovský Institute of Physical Chemistry, Academy of Sciences of the Czech Republic, Dolejškova 3, 128 23 Prague 8, Czech Republic

ARTICLE INFO

Article history:
Received 11 August 2009
Received in revised form
26 November 2009
Accepted 7 December 2009
Available online 14 December 2009

Keywords:
Neonicotionoid pesticides
Photocatalysis
Ozonation
Iron
Surface area

ABSTRACT

Combining TiO_2 photocatalysis with inorganic oxidants (such as O_3 and H_2O_2) or transition metal ions (Fe^{3+}, Cu^{2+} and Ag^+) often leads to a synergic effect. Electron transfer between TiO_2 and the oxidant is usually involved. Accordingly, the degree of synergy could be influenced by TiO_2 surface area. With this in mind, the disappearance of thiacloprid, a neonicotinoid insecticide, was studied applying various photochemical AOPs and different TiO_2 photocatalysts. In photocatalytic ozonation experiments, synergic effect of three different TiO_2 photocatalysts was quantified. Higher surface area resulted in a more pronounced synergic effect but an increasing amount of TiO_2 did not influence the degree of the synergy. This supports the theory that the synergy is a consequence of adsorption of ozone on the TiO_2 surface. No synergy was observed in photocatalytic degradation of thiacloprid in the presence of dissolved iron(III) species performed under varied experimental conditions (concentration, age of iron(III) solution, different TiO_2 films, usage of TiO_2 slurries). This goes against the literature for different organic compounds (i.e., monuron). It indicates different roles of iron(III) in the photodegradation of different organic molecules. Moreover, TiO_2 surface area did not affect photodegradation efficiency in iron(III)-based experiments which could confirm absence of electron transfer between TiO_2 photocatalyst and iron(III).

1. Introduction

Neonicotinoid insecticides represent the fastest growing class of insecticides introduced in the market since the launch of pyrethoids. Imidacloprid, a member of the first generation of neonicotinoids, is the top-selling insecticide worldwide [1], while thiacloprid belongs to the second generation of neonicotinoid insecticides and is replacing the members of the first generation. Both of them are among the active substances authorised for use in plant protection products (Annex I of Council Directive 91/414/EEC). Studies of environmental stability of neonicotinoids were performed in the past [2] and it was shown that thiacloprid is resistant to degradation in water by hydrolysis at neutral or acidic pH values and also considerable photostability was observed under simulated solar irradiation [3]. Since thiacloprid exhibits a possible high threat for aquatic systems, already proven by some ecotoxicological studies [4,5], it is of great importance to find an effective method for its elimination from aquatic systems. Advanced oxidation processes (AOPs) have been reported as the appropriate methods for this task. TiO_2 photocatalysis (O_2/TiO_2/UV) belongs to AOPs and has the potential of removing the organic pollutants from wastewater, although it is still not used in practice because of the low efficiency of the process [6]. A combination of photocatalysis together with ozone or ferric ions often increases the efficiency of the mineralization of organic compounds considerably due to additional reactions, which lead to a higher amount of highly reactive oxygen-based radicals [7,8].

The synergic effect of combining TiO_2 photocatalysis with the oxidants, such as O_3, H_2O_2, etc., or with transition metal ions, such as Fe^{3+}, Cu^{2+}, Ag^+, etc. is not a consequence of one simple chemical reaction or physical process but it results from a series of different reactions, which are often conditioned one by another. Some possible reasons for the synergic effects of ozonation coupled with UV radiation (O_3/UV) and O_2/TiO_2/UV have been proposed. First, ozone adsorbs on the surface of TiO_2 due to different interactions with TiO_2 surface such as (i) physical adsorption; (ii) formation of weak hydrogen bonds with surface hydroxyl groups; (iii) molecular or dissociative adsorption into Lewis acid sites [9]. Because it is a

Abbreviations: AOP, advanced oxidation process; O_3/UV, ozonation, coupled with UV radiation; O_2/TiO_2/UV, photocatalysis; O_3/TiO_2/UV, photocatalytic ozonation; Fe^{3+}/UV, irradiated iron(III) solution; Fe^{3+}/TiO_2/UV, combined TiO_2 photocatalysis with iron(III); Films P, Degussa P25 particulate films; Films D, sol–gel produced films without the addition of surfactant in the sol; Films C, sol–gel produced films with the addition of surfactant in the sol; *k*, degradation rate constant.

* Corresponding author at: Laboratory for Environmental Research, University of Nova Gorica, P.O. Box 301, Vipavska 13, SI-5001 Nova Gorica, Slovenia.
Tel.: +386 5 33 15 328; fax: +386 5 33 15 296.
E-mail addresses: urh.cernigoj@p-ng.si (U. Černigoj), urska.lavrencic@p-ng.si (U.L. Štangar), jaromir.jirkovsky@jh-inst.cas.cz (J. Jirkovský).

0304-3894/$ – see front matter © 2009 Elsevier B.V. All rights reserved.
doi:10.1016/j.jhazmat.2009.12.046

stronger oxidant than oxygen, it is – when adsorbed on the surface – more easily reduced by a photogenerated conduction electron from TiO_2 (Eqs. (1) and (2)), producing ozonide radical anion, which in the next steps generates a hydroxyl radical (Eqs. (3) and (4)) [10]. Also the recombination between holes and electrons is minimized due to the more efficient trapping of photogenerated electrons by ozone.

$$TiO_2 + h\nu \rightarrow TiO_2(e^- + h^+) \quad (1)$$

$$O_3 + TiO_2(e^-) \rightarrow O_3{}^{-\bullet} + TiO_2 \quad (2)$$

$$O_3{}^{-\bullet} + H^+ \rightarrow HO_3{}^{\bullet} \quad (3)$$

$$HO_3{}^{\bullet} \rightarrow O_2 + HO^{\bullet} \quad (4)$$

Moreover, even if molecular oxygen accepts the photogenerated electron, the resulting superoxide radical anion can react with ozone to give hydroxyl radical in consecutive steps (Eqs. (3)–(6)) [11].

$$O_2 + TiO_2(e^-) \rightarrow O_2{}^{-\bullet} + TiO_2 \quad (5)$$

$$O_2{}^{-\bullet} + O_3 \rightarrow O_3{}^{-\bullet} + O_2 \quad (6)$$

Also, ozone can react with H_2O_2 (or with the conjugated base of H_2O_2) (Eq. (7)), which is produced when molecular oxygen is reduced on the TiO_2 surface. Once more, ozonide radical anion is generated undergoing consecutive reactions to $HO^{\bullet}$ formation [12].

$$O_3 + HO_2{}^- \rightarrow O_3{}^{-\bullet} + HO_2{}^{\bullet} \quad (7)$$

Additionally, O_3/TiO_2/UV process is influenced by the ozone itself. In our previous study [3], it was shown that the synergy between ozonation and photocatalysis depends on the ozone dosage as well as on the pH of the aqueous solution. In another study of Beltran et al. [13], the effect of radical scavengers on synergy between photocatalysis and ozonation was also studied and the loss of synergy was a result of the scavengers which adsorb on the TiO_2 surface.

The synergic mechanism in the case of combining photocatalysis with transition metal ions shares some common features with photocatalytic ozonation (O_3/TiO_2/UV), but first of all, the iron system are even more pH dependant than ozone-based systems. In the case of added iron(III) ions in the TiO_2 photocatalytic system (Fe^{3+}/TiO_2/UV), the synergic effect observed could be explained by interactions between iron species and TiO_2 [14].

There are three parallel processes of $HO^{\bullet}$ generation in the system which include the iron species. One is a photocleavage of iron(III) hydroxoaqua complex (Eq. (8)), the second is a reduction of photogenerated TiO_2 holes by ferrous ions returning the photoactive iron(III) hydroxoaqua complexes and the third is a dark Fenton reaction (Eq. (9)) [15].

$$Fe(OH)^{2+} + h\nu \rightarrow Fe^{2+} + HO^{\bullet} \quad (8)$$

$$Fe^{2+} + H_2O_2 + H^+ \rightarrow Fe^{3+} + HO^{\bullet} + H_2O \quad (9)$$

$$Fe^{3+} + TiO_2(e^-) \rightarrow Fe^{2+} + TiO_2 \quad (10)$$

The reaction of adsorbed iron(III) with the photogenerated electrons (Eq. (10)) lowers the recombination rate of photogenerated holes and electrons perhaps resulting in an enhancement of the concentration of $HO^{\bullet}$ radicals [16]. But it appears that this way of $HO^{\bullet}$ production is less efficient than the direct formation via Eq. (8) and the synergy of the combined system is lost. On the contrary, the electron trapping by the soluble iron(III) aggregates has a positive influence on the synergy because such species are easily reduced on the TiO_2 surface, but at the same time they are not efficiently photodissociated in a way presented by Eq. (8). Additionally, the synergy is also affected by the concentration of TiO_2, iron species and other parameters, but the tendency of synergy with changing these parameters depends on the system studied and the general conclusions are difficult to summarize [17,18]. In a detailed study, conducted by Meštankova et al. [19], it was shown that it is possible to use more than a 10 times lower concentration of TiO_2 photocatalyst in the presence of iron(III) salt to reach the same photodegradation rate of monuron (a phenylurea herbicide) as for the corresponding single TiO_2 system.

It is well evidenced that in the O_3/TiO_2/UV as well as in the Fe^{3+}/TiO_2/UV process, the adsorption of the ozone or iron(III) on the titania surface are the key reactions leading to synergy. Therefore, it seems reasonable that the surface area of the catalyst plays an important role in the degree of synergy. Surprisingly, according to our knowledge, nobody has yet studied the effect of this parameter. For that reason, we investigated the disappearance of thiacloprid applying different AOPs (O_3/UV, O_3/TiO_2/UV, O_2/TiO_2/UV, irradiated iron(III) solutions (Fe^{3+}/UV) and Fe^{3+}/TiO_2/UV). The effect of the surface area was evaluated by using three different photocatalysts.

2. Experimental

2.1. Chemicals, preparation of sols and deposition of TiO_2 thin films

The chemicals in this study were used as purchased: acetonitrile (HPLC grade), tetraethoxysilane, concentrated sulphuric(VI) acid, 70% perchloric acid and 65% nitric(V) acid from J. T. Baker; titanium(IV) isopropoxide ($Ti(OiPr)_4$), potassium oxalate, sodium bicarbonate and 2-methoxyethanol from Fluka; Pluronic F-127 from Sigma, ferric perchlorate and 1,10-phenanthroline from Aldrich; 96% ethanol, ferrous sulphate(VI), sodium acetate, ammonium acetate, sodium thiosulphate, potasium iodide, sodium hydroxide, hydrochloric acid and ethyl acetoacetate (EAA) from Riedel-de Haen. All aqueous solutions of the organic pollutants were prepared by using highly pure water ($18\,M\Omega\,cm^{-1}$) from the NANOpure system (Barnstead). Pure thiacloprid was obtained from the commercial technical product Calypso SC 480 (Bayer) according to the procedure described in our previous publication [3]. Degussa P25 was provided by Degussa AG (Germany).

2.2. Thin film preparation and photoreactor set up

Transparent TiO_2–anatase films deposited on both sides of SiO_2-precoated soda-lime glass slides (190 mm × 12.5 mm × 2 mm) were produced by sol–gel processing route. Additionally, non-transparent Degussa P25 films were also deposited on soda-lime glass slides (dimensions of 190 mm × 12.5 mm × 2 mm) by dip-coating from the ethanolic suspension of Degussa P25 ($10\,g\,L^{-1}$). The detailed procedure of preparing of all the immobilized TiO_2 samples is described in our previous publication [20]. The names of the TiO_2 samples are composed of two characters: (1) D, C or P = the symbol of the type of titania where D represents the catalyst prepared from the sol without added surfactant; C represents the catalyst prepared from the sol with added surfactant Pluronic F-127 in the sol; P represents the Degussa P25 samples; (2) 1–4 = number of dipping-heating cycles.

A thorough materials characterization for all types of films was done previously [21–23]. In Table 1, their most important characteristics are collected. The material properties of Degussa P25 are taken from manufacturer data.

The reactor cell consists of a DURAN glass tube (240 mm, inner diameter 40 mm) which is closed on the lower side with a glass frit and a valve for gas purging. The effective volume of the glass tube is 250 mL. Eleven glass slides with or without immobilized catalyst were fastened radially on the spinning basket which fits in the tube. 6 low-pressure mercury fluorescent lamps (CLEO 20

Table 1
Characteristics of TiO_2 thin films prepared.

Characterization	Film D	Film C	Film P
Crystalline phase	Anatase	Anatase	Anatase:rutile = 70:30
BET surface area [$m^2\ g^{-1}$]	5.5	75	50–65
The size of primary particles [nm]	19	10	21
Macroscopic density of the deposited TiO_2 layer [$g\ cm^{-3}$]	4.3	2.2	Not possible to measure
Surface roughness [nm]	0.95	1.87	Not possible to measure
True absorption of UVA radiation by the thin film samples at 365 nm (the area density of TiO_2 100 $\mu g\ cm^{-2}$) [%]	9	9.5	28

W, 438 mm × 26 mm, Philips; broad maximum at 355 nm) were used as a UVA radiation source. A detailed scheme of the tube has been presented before [20]. The photon flux in the cell was evaluated by potassium ferrioxalate actinometry, and determined to be 4.2×10^{-5} einstein $L^{-1}\ s^{-1}$.

Ozone or oxygen were bubbled into the bottom of the reactor through the glass frit. Ozone was generated by Pacific Ozone Technology equipment (model LAB21) fed with pure oxygen (99.5%) and its gaseous concentration was determined by iodometric titration. The applied specific ozone dose for the experimental time of 30 min varied from 0.75 mg ozone per 1 mg of the pollutant (at the flow rate of ozone 0.00125 g min^{-1}) to 11.4 mg ozone per 1 mg of the pollutant (at the flow rate of ozone 0.019 g min^{-1}). The total gas flow rate was constant (0.17 L min^{-1}) during the experiment.

2.3. Degradation experiments

2.3.1. Ozone-based experiments

Thiacloprid solutions (100 mL, 2.0×10^{-4} M) were used in degradation experiments. The starting pH of the aqueous solution was regulated by adding perchloric acid to the value of 3.2. The temperature was kept constant at 30 °C during the experiment. The samples (4 mL) were taken from the cell at different times during the irradiation for HPLC analysis. The sample was purged with Ar for 5 min immediately after the withdrawal from the reactor cell to remove the excessive dissolved ozone. They were analyzed without additional filtration, extraction or centrifugation. The degradation experiments lasted between 15 and 45 min. At least two repetitions with each configuration were performed to evaluate the reproducibility of the measurements. After the experiment, the reactor cell and the spinning basket with the films were washed with deionised water (DI water). Before starting the next one, the cell was thoroughly washed and filled with the new pesticide solution. Some experimental specifications of each type of experiment are as follows.

O_3/UV: The pesticide solution was exposed to UVA radiation under constant purging with a mixture of oxygen and ozone. O_2/TiO_2/UV and O_3/TiO_2/UV experiments were performed with eleven glass slides coated with TiO_2 on both sides under otherwise similar irradiation conditions as in the O_3/UV process.

2.3.2. Iron(III)-based experiments

Firstly, the thiacloprid was dissolved in DI water (2.0×10^{-4} M). Depending on the experiment, the prepared solution was left untouched or was acidified to an appropriate pH value using a perchloric acid before dissolving different amounts of ferric perchlorate. After the addition of ferric perchlorate, the solution was aged from 0 min to 24 h, depending on the type of iron(III) condensation complex which was studied in the degradation experiment. The solution (100 mL) was then transferred into the reactor cell with the TiO_2 thin films and left for half an hour in darkness. Afterwards the irradiation started. In all experiments, the constant purging with oxygen was applied (0.17 L min^{-1}). A withdrawal of the samples and their preparation for HPLC analysis was done in the same way as it is described in Section 2.3.1. UV–vis absorption spectra of some of the iron species containing solutions were recorded on HP 8453 UV–vis spectrophotometer.

In some cases, the Fe^{3+}/TiO_2/UV experiments were not performed using TiO_2 thin films, but using the Degussa P25 slurry instead. In such case, an appropriate amount of the catalyst was suspended in the mixture of the thiacloprid and ferric perchlorate in DI water. The suspension was put in an ultrasound bath for 10 min and then left in darkness for additional 20 min before starting the irradiation. The samples taken for HPLC analysis were firstly centrifuged at 13200 rpm for 15 min and then the supernatant was collected for chromatographic analysis.

In all iron-based experiments, the reactor cell was thoroughly washed with 3 M sulphuric acid after the degradation experiments to remove the adsorbed iron species from the glass surface. A usual washing with DI water followed after treating the glassware with sulphuric acid.

2.4. Analytical procedure

The HPLC analyses were made on a HP 1100 Series chromatograph coupled with a DAD detector. The chromatographic separations were run on a C8 column (Kromasil 100, 250 mm × 4.6 mm, 5 μm) using a 85:15 mixture of aqueous ammonium acetate (10 mM) and acetonitrile as the eluent in the first 4 min, then it was changed into a 30:70 mixture by applying a linear gradient between 4 and 16 min. The flow rate was 1.0 mL min^{-1}. The injection volume was 10 μL. Thiacloprid was monitored by DAD detector at 242 nm.

3. Results and discussion

Photocatalytic activities of C and D films made via sol–gel route have been recently evaluated by the in situ measurement of the bleaching of Plasmocorinth B aqueous solutions [21] and also by measuring the quantum yields of the coumarin degradation and of 7-hydroxycoumarin formation [23]. The characteristics of the prepared films are therefore well-known as well as their correlation to photocatalytic activities. Additionally, the degradation of thiacloprid using photocatalysis, ozonation and photocatalytic ozonation has already been investigated, but only using Degussa P25 films and different C films [3]. A detailed description of a photocatalytic reactor has been published recently [20]. Accordingly, the experimental conditions were set according to our previous studies. Because the mineralization process and the evolution of inorganic ions in the applied degradation experiments have been already performed in our previous study [3], only HPLC analysis was used as an analytical tool in this work to evaluate the effect of the photocatalyst surface area on the rate of the degradation reaction. All different experimental configurations of photocatalytic systems are collected in Table 2.

3.1. Ozone-based experiments

The ozone-based experiments were performed first. The pH of the solution was chosen to be acidic because we already showed

Table 2
Configuration of photocatalysts, their amount and concentration.

Configuration	Catalyst	Average amount of TiO_2 on 11 slides [mg]	Weight concentration of TiO_2 in the solution of pollutant [mg L^{-1}]
C1	Films C	25	100
D2	Films D	25	100
C4	Films C	100	400
D4	Films D	50	200
P4	P25	84	340
Slurry	P25	–	26

that the synergy is the most pronounced at acidic pHs [3] and because the decomposition of ozone molecules in the reaction with hydroxide ions is diminished at such pH values. The perchloric acid was chosen to acidify the aqueous solution of thiacloprid because perchlorate is known not be adsorbed on the titania surface and it also does not react with all the oxidative species generated during the degradation experiments [17]. In all experiments performed, the initial pH was fixed to 3.2 and the final pH after the degradation varied between 2.9 and 3.2. This small change should not influence the possible changes in the kinetics of thiacloprid degradation. The amount of the dissolved ozone was kept constant during the whole degradation experiments by the continuous purging the reaction cell with a mixture of ozone and oxygen. Keeping the concentration of dissolved ozone constant all the time simplifies the following calculations.

Fig. 1 presents three different experiments of the degradation of thiacloprid aqueous solution, namely O_3/UV, O_2/TiO_2/UV and O_3/TiO_2/UV. The C1 films were used in the specified experiment and ozone flow rate was fixed to 0.0055 g min^{-1}. Similarly, the experiments with other photocatalytic configurations and the other ozone dosages were performed and all the data were collected and analyzed. The O_2/TiO_2/UV experiment formally followed the first-order degradation kinetics and was therefore fitted as such. On the contrary, the O_3/UV degradation followed the zero-order kinetics until the concentration of thiacloprid decreases below one-fourth of the initial concentration regardless of the concentration of ozone used. Therefore, the data of the concentration of thiacloprid below one-fourth of the initial concentration were not used for fitting a zero-order kinetic equation. The third degradation curve belongs to the photocatalytic ozonation experiment. Evidently, the photocatalytic ozonation was the most effective way to degrade thiacloprid but the synergy has also to be calculated theoretically from the obtained results. If there is no synergy between the

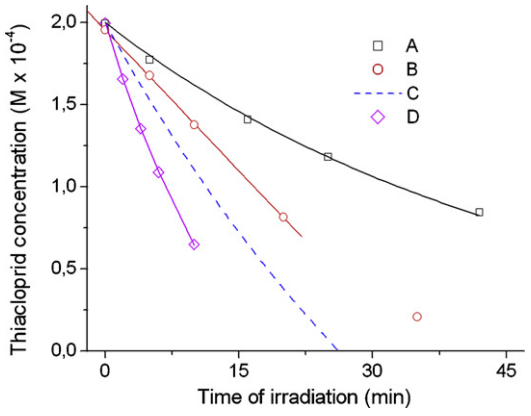

Fig. 1. Plots of thiacloprid concentration (M) versus irradiation time (min) for degradation of thiacloprid under the following conditions: pH 3.2, 11 glass slides with immobilized C1 TiO_2 thin layers, the flow rate of ozone 0.0055 g min^{-1} and the flow rate of the purging gas (oxygen or mixture of ozone and oxygen) 0.17 L min^{-1}—(□) A: O_2/TiO_2/UV; (○) B: O_3/UV; (▬ ▬ ▬) C: theoretical sum of separate O_3/UV and O_2/TiO_2/UV; (◇) D: O_3/TiO_2/UV. (For interpretation of the references to color in this figure legend, the reader is referred to the web version of the article.)

O_3/UV and O_2/TiO_2/UV process, the sum of the individual degradation fittings should result in a curve which fits with the data of the O_3/TiO_2/UV process. An Eq. (11) is obtained by combining the zero-order kinetics with the first-order kinetics for the compound degradation:

$$c = c_0 e^{-kt} + \frac{k_1}{k}(e^{-kt} - 1) \quad (11)$$

c_0 represents an initial concentration of thiacloprid, k is a first-order degradation rate constant of thiacloprid in O_2/TiO_2/UV process while k_1 is a zero-order degradation rate constant of thiacloprid in O_3/UV process. If the calculated values of k and k_1 are inserted in Eq. (11), a simulated curve is obtained presenting the sum of both studied processes. Obviously from Fig. 1, the sum of O_3/UV and O_2/TiO_2/UV processes is less effective for thiacloprid degradation than the $O_3/UV/TiO_2$ process. The difference between these two sets of data is attributed to a synergic effect between the ozonation and photocatalysis. In the next step, the $O_3/UV/TiO_2$ experimental data were fitted using Eq. (11), where the value of k_1 was taken the same as in O_3/UV experiment because it was supposed that the contribution of the O_3/UV degradation process to the total degradation of thiacloprid was the same in the O_3/UV as well as in the $O_3/UV/TiO_2$ experiments. The new value of k, obtained from fitting $O_3/UV/TiO_2$ is the first-order degradation rate constant of thiacloprid in the $O_3/UV/TiO_2$ process, and its value is higher than the value of k in the corresponding O_2/TiO_2/UV process due to the synergic effect. As it is seen from Fig. 1, the fitted curve with the new k undoubtedly matches the experimental data in the initial steps of degradation.

For the C1 films, the synergic effect was evident with all applied concentrations of ozone. The next step was to find out if changing the type of catalyst influences the degree of synergy. Therefore, the D2 films were investigated. It is important to notice that these two types of catalysts were prepared in completely the same way and the only difference was the addition of a surfactant in the preparation procedure of C films. The addition of surfactant increases the porosity of the film and also the surface roughness and surface area of the catalyst and this is the main difference between these two types of catalyst. Accordingly, the conditions of deposition were chosen in a way that the same amount of TiO_2 was deposited in the C1 and D2 thin films. Also, the same true absorption characteristics in UV region per amount of TiO_2 were measured for these two types of films (Table 2). It is already known from previous studies [21,23] that these two configurations have exactly the same photocatalytic activities for the degradation of compounds which are not adsorbed on the surface of titania. Under these conditions, the hydroxyl radical attack initiates the degradation instead of the direct hole transfer.

Because it is supposed that the adsorption of ozone molecules on the titania surface is one of the main reasons for the synergy between photocatalysis and ozonation, it was expected that the synergy should be more pronounced with the films having higher surface area (i.e., C1 films). In Fig. 2, the relationship between the fitted rate constants k in O_3/TiO_2/UV process and the flow rate of ozone is shown. C1 and D2 films are compared in Fig. 2. Firstly, the value of k increases with the increase of the ozone flow rate

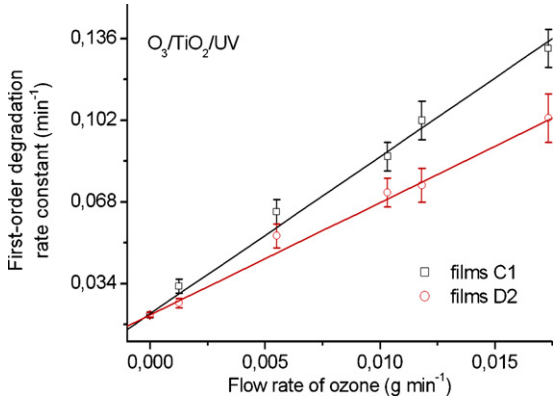

Fig. 2. Plots of the first-order disappearance rate constant of thiacloprid (min^{-1}) versus the ozone flow rate ($g\,min^{-1}$) for two different photocatalysts, namely C1 and D2. The concentration of TiO_2 was in both cases the same ($100\,mg\,L^{-1}$). The initial concentration of thiacloprid was 2.0×10^{-4} M, the pH of solution was 3.2, a flow rate of the purging gas was $0.17\,L\,min^{-1}$.

which means that the synergy is higher with the increase of the dissolved ozone concentration. This could be explained with the higher coverage of the titania surface with the ozone molecules at higher concentrations of dissolved ozone. Consequently, a higher synergy is also expected. The dependence between k and the ozone flow rate is linear; therefore, the data were fitted and a line with the characteristic slope was obtained. Secondly, when the concentration of ozone is 0 (O_2/TiO_2/UV experiment), films D2 as well as films C1 show the same photocatalytic activity for the degradation of thiacloprid. Thirdly, the slopes of the line for films C1 is steeper than for films D2. The slope of the line C was calculated to be $6.5\,g^{-1}$ and the slope of the line D was calculated to be $4.5\,g^{-1}$. Because the positive slope of the line is an indication of the synergy (slope 0 would mean no synergy), it could be further concluded that the steeper slope coincides with the higher synergy between the ozonation and photocatalysis. This supports the hypothesis that despite the same activity of the D2 and C1 films in O_2/TiO_2/UV experiments, the ozone has a higher beneficial effect when the films with a higher surface area are used. The more ozone molecules are adsorbed to the C1 titania surface the more photogenerated electrons are scavenged by the ozone and the more photogenerated holes are available for the reaction with the adsorbed water on the one side and the more ozonide radical anions are produced on the other side.

In the next step, the C4 and D4 films were investigated. The C4 films contain 4 times higher amount of TiO_2 compared to C1, because there are four layers of sol C deposited. Similarly, film D4 contains 2 times higher amount of TiO_2 compared to the D2 films. The surface areas of both configurations (C4 and D4) should be comparable to the surface areas of the C1 and D2 films, because the catalyst itself should not be changed just due to increase of the thickness. In both cases (with C4 and D4), a higher activity toward thiacloprid degradation was expected in the O_2/TiO_2/UV experiment due to the higher amount of deposited TiO_2, but the synergy after the addition of ozone should be comparable with the synergy in the corresponding system with the lower amount of the same catalyst. In other words, the fitted lines of the similar data as presented in Fig. 2 should have the same slope but a different intersection with the y-axis. Fig. 3A compares the C1 and C4 systems, while Fig. 3B compares the D2 and D4 films. It is evident in both cases that in the absence of ozone, the higher amount of deposited TiO_2 results in a higher photocatalytic degradation rate. It was surprising that the increase of the activity was lower than expected. In our previous study, of a classical photocatalytic degradation (O_2/TiO_2/UV) of coumarin [23], the C4 films were

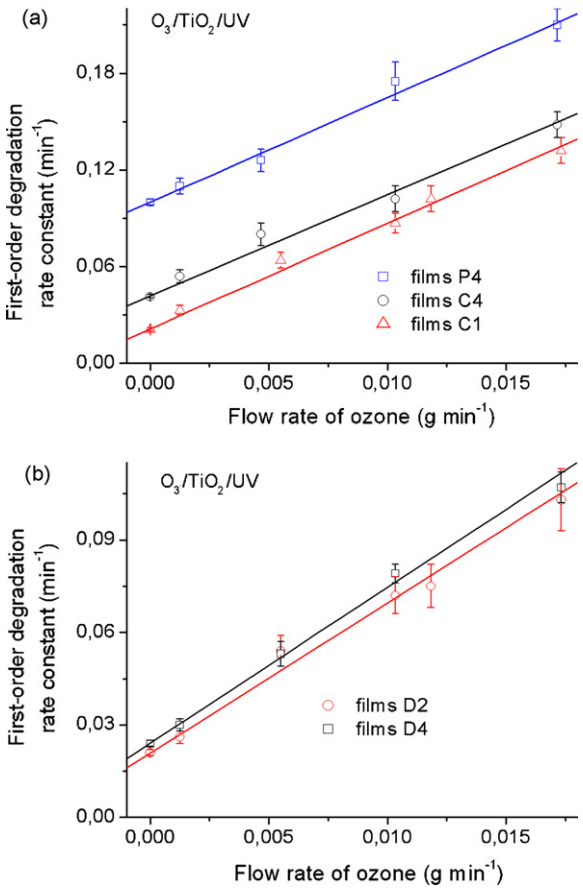

Fig. 3. Plots of the first-order disappearance rate constant of thiacloprid (min^{-1}) versus the ozone flow rate ($g\,min^{-1}$) for three different photocatalysts with different concentrations of TiO_2 in the solution. The initial concentration of thiacloprid was 2.0×10^{-4} M, the pH of solution was 3.2, a flow rate of the purging gas was $0.17\,L\,min^{-1}$. (A) Comparison between C1 and C4 and P4 TiO_2 thin layers. (B) Comparison between D2 and D4 TiO_2 thin layers.

approximately 3 times higher photoactive than the C1, and the D4 films were approximately 2 times more photoactive than the D2 films. The differences are not so clear in the present study, particularly because the C4 films are only twice more active than the C1, and the D4 films are just 1.2 times better than D2. The reasons could be due from the different reaction conditions used in the present and previous investigation (the light source used, reactor system, type of the molecule, pH of the solution). However, it is not our intention to find the answer to this question, because the synergy between ozonation and photocatalysis is our present interest. Fig. 3 supports the hypothesis that the synergy keeps the same value if higher amount of the same catalyst is irradiated. In other words, the slope of the line D4 has a value of $4.9\,g^{-1}$ what is comparable with the slope of the line D2 ($4.5\,g^{-1}$). The same is confirmed also for the C samples, where the slope of the C4 line is $6.3\,g^{-1}$ which is comparable with the value $6.5\,g^{-1}$, i.e., the value of the slope of the line obtained from the C1 films. All these results represent additional proof that the synergy between ozonation and photocatalysis is based on the degree of the adsorption of ozone molecules over the titania surface and that a higher surface area increases the degree of synergy regardless of the usual photocatalytic activity of the sample.

Additionally, the same set of experiments was performed using the Degussa P25 films (P films). These films are non-transparent because they are particulate films with different characteristics other than the C or D films (Tables 1 and 2). The photocatalytic activity per amount of irradiated catalyst of Degussa P25 is considerably

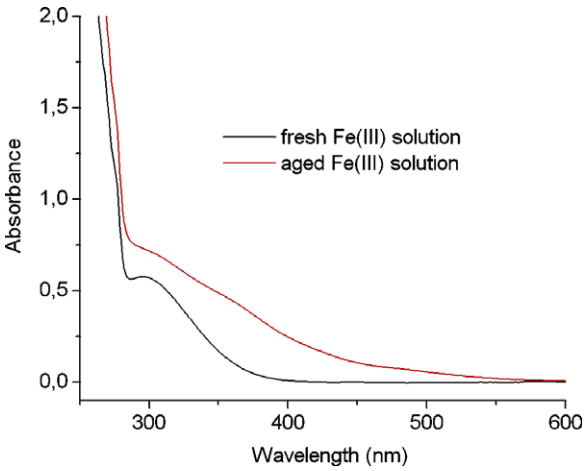

Fig. 4. UV–vis absorption spectra of fresh and 17 h aged aqueous solution of a mixture of thiacloprid (2.0×10^{-4} M) and ferric perchlorate (4.1×10^{-5} M).

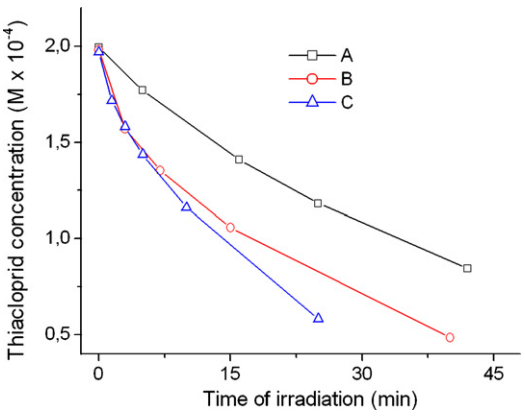

Fig. 5. Plots of thiacloprid concentration (M) versus irradiation time (min) for degradation of thiacloprid under the following conditions: pH 3.2. 11 glass slides with immobilized C1 TiO_2 thin layers and a fresh solution of ferric perchlorate (4.1×10^{-5} M) were used in the appropriate experiments. (□) A: O_2/TiO_2/UV; (○) B: Fe^{3+}/UV; (Δ) C: Fe^{3+}/TiO_2/UV. (For interpretation of the references to color in this figure legend, the reader is referred to the web version of the article.)

higher than in the case of the C and D films which were described in our previous publication [23]. In our experiments, the P4 films with the area density of Degussa P25 145 μg cm^{-2} were used that is approximately 10% less than in the case of C4 films. Despite a similar amount of irradiated catalyst in both cases (100 and 84 mg), the P4 films show 2.4 times higher photocatalytic activity in O_2/TiO_2/UV compared to C4 films towards thiacloprid degradation. Despite all distinctive differences between the catalysts, the BET surface area of Degussa P25 powder is between 50 and 65 $m^2\,g^{-1}$, close to the BET surface area of the C films. Therefore, also a similar degree of synergy between ozonation and photocatalysis was expected between the C and P films. Indeed, the synergy measured by the slope of the P4 line (6.6 g^{-1}) is comparable with the slope of the C1 or C4 lines (6.5 and 6.3 g^{-1}) despite the higher photocatalytic activity of the P4 films (Fig. 3A). It is evident that the surface area affects the degree of synergy between ozonation and photocatalysis more than the catalytic properties of the photocatalyst. These observations also have the future consequences if such materials will be used once in real applications. When combining photocatalysis with ozonation, it is beneficial to prepare not only a very photocatalytically active catalyst, but also a catalyst with a high surface area.

3.2. Iron(III)-based experiments

First, a fresh solution of iron(III) ions and thiacloprid in slightly acidified water (pH 3.1 using $HClO_4$) was irradiated to observe the kinetics of the degradation in Fe^{3+}/UV system. No TiO_2 films were used in these experiments. The primary iron(III) complex, which is formed just after the dissolution of ferric perchlorate, absorbs the radiation in the UVB and UVA part of the spectrum with the broad maximum at 300 nm. The UV–vis spectrum of such solution is shown in Fig. 4 (fresh iron(III) solution) where the maximum at 300 nm is well observed . The primary iron(III) complex $Fe(OH)^{2+}$ is not stable and condenses to other complexes which are not so photoactive and which possess different absorption characteristics than $Fe(OH)^{2+}$. The red shift of the absorption is proof of aggregated iron(III) complexes, which occur in an aged iron(III) solution (17 h aged solution in Fig. 4). An acidification with $HClO_4$ prevents the aggregation of the primary iron(III) complex which is consequently stable for a longer time. At a lower pH of the solution (additional acidification of the solution with $HClO_4$), therefore, no difference in the UV/vis spectra of the solution just after the dissolution of iron(III) and after 17 h of aging was observed (not shown in the figure). The main mechanism of the photoproduction of hydroxyl radicals in Fe^{3+}/UV experiments, where fresh iron(III) was used, is presented with the Eq. (8). The condensed iron(III) complexes are far less photoactive.

In the next experiments, the TiO_2 thin films were included in the Fe^{3+}/UV process (Fe^{3+}/TiO_2/UV). The experiments were performed in a similar way as the Fe^{3+}/UV photodegradations, the only difference was the addition of the TiO_2 films. The fresh solution of iron(III) ions with the additional acidification by $HClO_4$ to pH 3.1 enabled the $Fe(OH)^{2+}$ complex to be the main source of iron(III). In order to evaluate the effect of the concentration of the dissolved iron(III) on the degradation efficiency, different concentrations of the initial iron(III) ions were also tested. An example of a series of experiments with the concentration of dissolved iron(III) set at 2.3 mg L^{-1} is shown in Fig. 5. In the initial steps of the irradiation experiment, when the concentration of dissolved primary iron(III) complex was still high, a reaction followed a pseudo-first-order degradation pattern. With decreasing the concentration of iron(III) in the solution due to Eq. (8), the disappearance rate of thiacloprid decreased, which is proof that the iron(II) is not efficiently recovered back to iron(III), as is well-known from the literature [17]. Therefore, only the data of an initial degradation of thiacloprid were used for fitting a first-order kinetic equation. Thus the calculated rate constants of thiacloprid degradation partly characterize both kinetic stages before and after reaching the photostationary equilibrium between Fe(III) and Fe(II) which is established only after some irradiation time. It would be better to use the degradation constants under equilibrium conditions, but due to the complexity of such measurements we decided to use the “initial” degradation rate constants. For proving or disproving the potential synergy between titania and iron, they should be reasonably valid. The calculated values of the first-order rate constants for different processes (Fe^{3+}/UV, O_2/TiO_2/UV and Fe^{3+}/TiO_2/UV) and for different concentrations of iron(III) are summarized in Fig. 6. The most evident and general observation is an increase in the disappearance rate with the increase of the concentration of the initial iron(III) concentration which was expected due to a more efficient absorption of UV photons by a higher concentration of primary iron(III) complex.

If the sum of first-order disappearance rate constants of O_2/TiO_2/UV + Fe^{3+}/UV were smaller than disappearance rate constants of Fe^{3+}/TiO_2/UV, the synergic effect of iron(III) would be easily proven. Surprisingly, no synergy between O_2/TiO_2/UV and Fe^{3+}/UV was noticed regardless of the concentration of dissolved ferric ions. When evaluating the data of the P4 experiments, a sig-

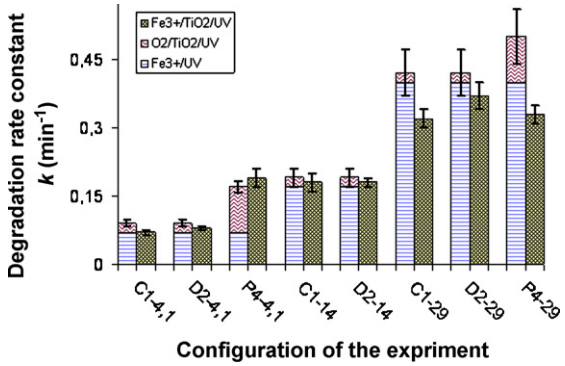

Fig. 6. Plots of calculated first-order degradation rate constants (min^{-1}) for Fe^{3+}/UV, O_2/TiO_2/UV and Fe^{3+}/TiO_2/UV experiments versus the concentration of ferric perchlorate (M, $\times 10^{-5}$) under the following conditions: fresh solution of ferric perchlorate and perchloric acid, the initial concentration of thiacloprid was 2.0×10^{-4} M, the pH of solution was 3.1, a flow rate of the purging oxygen was 0.17 L min^{-1}. Configuration of the particular experiment is given on X-axis as a symbol of the used TiO_2 layer (C1, D2 or P4) followed by an initial concentration of Fe(III) ions (4.1, 14 and 29×10^{-5} M).

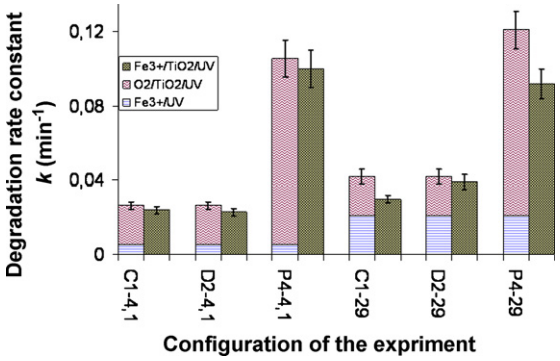

Fig. 7. Plots of calculated first-order degradation rate constants (min^{-1}) for Fe^{3+}/UV, O_2/TiO_2/UV and Fe^{3+}/TiO_2/UV experiments versus the concentration of ferric perchlorate (M) under the following conditions: aged solution of ferric perchlorate. The initial concentration of thiacloprid was 2.0×10^{-4} M, the pH of solution was between 3.2 and 4.0, a flow rate of the purging oxygen was 0.17 L min^{-1}. Configuration of the particular experiment is given on X-axis as a symbol of the used TiO_2 layer (C1, D2 or P4) followed by an initial concentration of Fe(III) ions (4.1 and 29×10^{-5} M).

nificant difference is the much higher activity of the P4 films in the O_2/TiO_2/UV process compared to C1 or D2 efficiency which resulted also in a higher efficiency of the overall Fe^{3+}/TiO_2/UV process. But still no synergy between Fe^{3+}/UV and O_2/TiO_2/UV was observed even with the P4 films.

No noticeable difference between the efficiencies of the D2 and C1 experiments (with different surface areas) was achieved. This makes sense if the degradation occurs mainly via iron(III) photoprocesses and if the reduction of iron(III) on the TiO_2 surface has a negligible effect in the whole degradation scheme. It is anticipated that due to a much better efficiency of a production of hydroxyl radicals in the iron(III) photoprocess compared to TiO_2 photocatalysis, the synergy between iron(III) ions and TiO_2 could not be observed, although it exists.

The deteriorating effect of the combined system on the efficiency of degradation is also noticed in all the experiments with the highest amount of dissolved iron(III) ions. It is believed that it is a consequence of the partial absorption of irradiation by the TiO_2 films and therefore the absorbed photons are not available to enter into the more efficient Fe^{3+}/UV process.

In the next step, the experimental conditions were changed to diminish the concentration of active $Fe(OH)^{2+}$ species. Aged iron(III) solutions were used instead of fresh iron(III) complexes. It is well-known that aged aqueous solutions of iron(III) have a lower photoactivity [17], however, such a system still contains iron(III) species capable of electron extraction from the conduction band of TiO_2.

Therefore, iron(III) perchlorate was dissolved in an aqueous solution of thiacloprid without previous acidification and such solution was aged for 17 h. An example of the UV–vis spectrum of the 17 h aged solution (without additional acidification) is shown in Fig. 4. The initial concentration of $Fe(OH)^{2+}$ complex (with the broad max. at 300 nm) decreased to below 10% [17]. The pH of the solution depended on the initial concentration of ferric perchlorate, but it was in the range between 3.4 and 4.2. Firstly, the Fe^{3+}/UV experiments were carried out. The initial degradation rates of thiacloprid were fitted as first-order degradation reactions and the corresponding rate constants are summarized in Fig. 7. As expected, the kinetics of the degradation were considerably slower than in case where the same concentration of fresh iron(III) was used (Figs. 6 and 7). This is a logical result if it is anticipated that condensed iron(III) species, which are the products of aging of the aqueous solution of ferric perchlorate, are not (or are weakly) photoactive.

The sum of the degradation rate constants of the separated processes (Fe^{3+}/UV and O_2/TiO_2/UV) were always higher or the same as the corresponding rate constant in the Fe^{3+}/TiO_2/UV experiment. Once again, no synergy between iron(III) and photocatalysis was observed regardless of the concentration of the dissolved ferric perchlorate and regardless of the catalyst used. At the same time, the deteriorating effect of iron(III) to the efficiency of the photocatalysis is not evident. It seems likely that both processes occur undependably from one to another.

Our last trial, with the intention to observe the synergy between the iron(III) and the TiO_2 photocatalysis, was a switch from an immobilized photocatalytic system to a slurry system. The contact between the liquid and solid state is much better in a slurry and a different behavior of the photocatalytic system was anticipated. A concentration of the Degussa P25 catalyst (25 mg L^{-1}) and of the ferric perchlorate (concentration of iron(III) 2.9×10^{-4} M) were the same as in the experiments conducted by Meštanková et al. [17], because the selected conditions led to the maximal synergic effect in their case. Experiments using a fresh solution as well as an aged solution of iron(III) were performed and the first-order degradation rate constants are collected in Fig. 8. Once again, no synergy was observed regardless of the degree of aggregation of the ferric species. Moreover, there is a small deteriorating effect in the experiments carried out with the fresh solution which could be explained due to the partial absorption of irradiation by the photochemically less efficient titania and consequently with a smaller number of absorbed photons by the $Fe(OH)^{2+}$ complex.

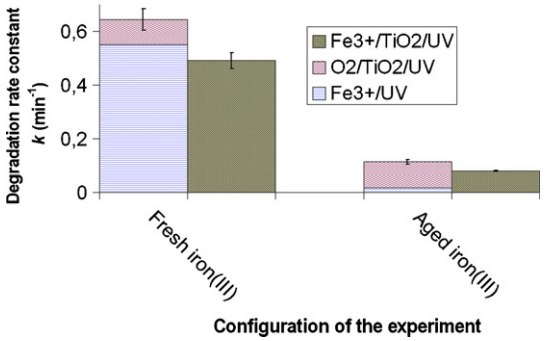

Fig. 8. : Plots of calculated first-order degradation rate constants (min^{-1}) for Fe^{3+}/UV and Fe^{3+}/TiO_2/UV experiments versus the concentration of ferric perchlorate (M) under following conditions: Degussa P25 suspensions (26 mg L^{-1}); fresh and aged solution of ferric perchlorate (2.9×10^{-4} M). The initial concentration of thiacloprid was 2.0×10^{-4} M, a flow rate of the purging oxygen was 0.17 L min^{-1}.

No synergy was observed in the degradation of thiacloprid with different iron-based advanced oxidation methods. There is no explanation according to the all known literature where a synergic effect of iron(III) on photocatalysis was observed. Additional and more detailed experiments, such as studying the adsorption of iron(III) to the catalyst's surface, performing experiments in anoxic conditions, monitoring the concentrations and types of iron species during the degradation, would explain the reasons for the absence of the synergy.

4. Conclusion

All the degradation methods applied are able to remove and destroy the thiacloprid molecules in water. A synergy between ozonation and TiO_2 photocatalysis of the degradation of thiacloprid was evident in the acidic solution. It was showed that a higher surface area of the catalyst resulted in a more pronounced synergic effect. An elegant way to quantify the synergic effect was to perform the O_3/TiO_2/UV experiments with different concentrations of dissolved ozone. An increasing amount of the same type of the catalyst did not influence the degree of synergy which is additional proof that a synergy is a consequence of the adsorption of the ozone molecule on the titania surface. Our intention for future research is to clarify the synergy between ozonation and photocatalysis of the degradation of various types organic molecules and prepare a catalyst with a synergic effect as high as possible.

No synergy between iron(III) and photocatalysis in combined iron/TiO_2 photosystems existed in photodegradation of thiacloprid regardless of the different experimental conditions used (concentration of iron(III), aging of iron(III), pH of the solution, various TiO_2 films, slurries, etc.). This was a surprise for us, but it seems that iron(III) does not play the same role as in the case of degradation of some other organic compounds (such as monuron). Moreover, no effect of the surface area of the photocatalyst in the efficiency of the degradation process was present in iron-based experiments, confirming the observations that no transfer of electrons between iron(III) and photocatalyst's surface area occurred.

Acknowledgements

We are very grateful to Degussa AG (Germany) for providing us P25 TiO_2 powder samples free of charge. This work was supported by the Ministry of Higher Education, Science and Technology of the Republic of Slovenia.

References

[1] P. Meienfisch, F. Brandl, W. Kobel, A. Rindlisbacher, R. Senn, Nicotinoid Insecticides and Nicotin Acetylholine Receptor, Springer, Tokyo, 1999.
[2] J. Krohn, Behaviour of thiacloprid in the environment, Planzenschutz-Nachrichten Bayer 54 (2001) 281–290.
[3] U. Černigoj, U. Lavrenčič Štangar, P. Trebše, Degradation of neonicotinoid insecticides by different advanced oxidation processes and studying the effect of ozone on TiO_2 photocatalysis, Appl. Catal. B: Environ. 75 (2007) 229–238.
[4] M.A. Beketov, M. Liess, Acute and delayed effects of the neonicotinoid insecticide thiacloprid on seven freshwater arthropods, Environ. Toxicol. Chem. 27 (2008) 461–470.
[5] M.A. Beketov, M. Liess, Variability of pesticide exposure in a stream mesocosm system: macrophyte-dominated vs. non-vegetated sections, Environ. Pollut. 156 (2008) 1364–1367.
[6] U.I. Gaya, A.H. Abdullah, Heterogeneous photocatalytic degradation of organic contaminants over titanium dioxide: A review of fundamentals, progress and problems, J. Photochem. Photobiol. C: Photochem. Rev. 9 (2008) 1–12.
[7] T.E. Agustina, H.M. Ang, V.K. Vareek, A review of synergic effect of photocatalysis and ozonation on wastewater treatment, J. Photochem. Photobiol. C: Photochem. Rev. 6 (2005) 264–273.
[8] M.I. Litter, Heterogeneous photocatalysis: transition metal ions in photocatalytic systems, Appl. Catal. B: Environ. 23 (1999) 89–114.
[9] M. Addamo, V. Augugliaro, E. Garcia-Lopez, V. Loddo, G. Marci, L. Palmisano, Oxidation of oxalate ion in aqueous suspensions of TiO_2 by photocatalysis and ozonation, Catal. Today 107–108 (2005) 612–618.
[10] M.D. Hernandez-Alonso, J.M. Coronado, A. Javier Maira, J. Soria, V. Loddo, V. Augugliaro, Ozone enhanced activity of aqueous titanium dioxide suspensions for photocatalytic oxidation of free cyanide ions, Appl. Catal. B: Environ. 39 (2002) 257–267.
[11] P. Kopf, E. Gilbert, S.H. Eberle, TiO_2 photocatalytic oxidation of monochloroacetic acid and pyridine: influence of ozone, J. Photochem. Photobiol. A: Chem. 136 (2000) 163–168.
[12] M.J. Farre, M.I. Franch, S. Malato, J.A. Ayllon, J. Peral, X. Domenech, Degradation of some biorecalcitrant pesticides by homogeneous and heterogeneous photocatalytic ozonation, Chemosphere 58 (2005) 1127–1133.
[13] F.J. Beltran, A. Aguinaco, J.F. Garcia-Araya, A. Oropesa, Ozone and photocatalytic processes to remove the antibiotic sulfamethoxazole from water, Water Res. 42 (2008) 3799–3808.
[14] M.S. Nahar, K. Hasegava, S. Kagaya, S. Kuroda, Adsorption and aggregation of Fe(III)–hydroxy complexes during the photodegradation of phenol using the iron-added-TiO_2 combined system, J. Hazard. Mater. 162 (2009) 351–355.
[15] H. Meštankova, G. Mailhot, J. Jirkovsky, J. Krysa, M. Bolte, Effect of iron speciation on the photodegradation of monuron in combined photocatalytic systems with immobilized or suspended TiO2, Environ. Chem. Lett. 7 (2009) 127–132.
[16] T. Ohno, D. Haga, K. Kaijaki, M. Matsumura, Unique effects of iron(III) ions on photocatalytic and photoelectrochemical properties of titanium dioxide, J. Phys. Chem. B 101 (1997) 6415–6419.
[17] S.W. Lam, K. Chiang, T.M. Lim, R. Amal, G.K.-C. Low, The role of ferric ion in the photochemical and photocatalytic oxidation of resorcinol, J. Catal. 234 (2005) 292–299.
[18] M. Mrowetz, E. Selli, Effects of iron species in the photocatalytic degradation of an azo dye in TiO_2 aqueous suspensions, J. Photochem. Photobiol. A: Chem. 162 (2004) 89–95.
[19] H. Meštankova, G. Mailhot, J. Jirkovsky, J. Krysa, M. Bolte, Mechanistic approach of the combined (iron–TiO_2) photocatalytic system for the degradation of pollutants in aqueous solution: an attempt to rationalisation, Appl. Catal. B: Environ. 57 (2005) 257–265.
[20] U. Černigoj, U. Lavrenčič Štangar, P. Trebše, Evaluation of a novel Carberry type photoreactor for the degradation of organic pollutants in water, J. Photochem. Photobiol. A: Chem. 188 (2007) 169–176.
[21] U. Černigoj, U. Lavrenčič Štangar, P. Trebše, P. Rebernik Ribič, Comparison of different characteristics of TiO_2 films and their photocatalytic properties, Acta Chim. Slov. 53 (2006) 29–35.
[22] U. Černigoj, U. Lavrenčič Štangar, P. Trebše, U. Opara Krašovec, S. Gross, Photocatalytically active TiO_2 thin films produced by surfactant-assisted sol–gel processing, Thin Solid Films 495 (2006) 327–332.
[23] U. Černigoj, U. Lavrenčič Štangar, P. Trebše, M. Sarakha, Determination of catalytic properties of TiO_2 coatings using aqueous solution of coumarin: standardization efforts, J. Photochem. Photobiol. A: Chem. 201 (2009) 142–150.